Journal of Rajasthan Academy of Physical Sciences
ISSN: 0972-6306; URL: http://raops.org.in
Vol.20, No.3&4, July-December, 2021, 207-218

WILLIAMSON FLUID FLOW OVER A STRETCHING CYLINDER WITH THERMAL CONDUCTIVITY AND HEAT GENERATION/ABSORPTION

Amala Olkha[1] and Amit Dadheech[2]
[1,2]Department of Mathematics, University of Rajasthan, Jaipur-302004, India
E-mail: [1]amalaolkha@gmail.com, [2]amitmyfr@gmail.com

Abstract: Present investigation examines flow of Williamson fluid across a stretching cylinder in a porous medium with thermal conductivity and heat generation/absorption. By utilizing relevant transformations acclimated PDE's are transmuted in ODE's. Arithmetic simulation is elucidated by exercising R-K 4th order technique along with shooting method in MATLAB syntax for temperature and momentum equations. The apprehensions of pictorial and tabular notations are used for porous medium parameter Kp, Weissenberg number We, Prandtl number Pr to analyses the impacts of physical parameters on velocity and energy. The analysis discovered that velocity profile is improved for Weissenberg number We, Heat generation/absorption parameter Q^* and thermal Conductivity ε and contrary effect can also be seen in the temperature profile for We, Pr, Kp. The obtained results confirm that an excellent agreement is achieved with those available in the literature.

Keyword: Williamson fluid, slip condition, Porous medium, stretching cylinder.

1. Introduction

Non-Newtonian fluid flows with its numerous features over porous cylinder has become a remarkable problem recently because it has significant role in industry, thermal energy investigation area. Significantly heat transfer problem is fascinated. Pseudoplastic fluids that exhibit both viscous and elastic characteristics, initially recognized by Williamson and established a set of equations, named Williamson model. The study of pseudoplastic fluids flow has become important now a days since its huge applications in the field of drawing of polymer sheets, photographic film production, melting of high molecular weight polymers etc. The Williamson model is analyzed by respective analyst covering several flow patterns and offers numerous examinations as its consequences. Bilal et al. [1] examined the Williamson fluid flow in three dimensions using a bi-directional non-linear stretching surface. They investigated and discovered that for large values of both non-linearity and Williamson parameter, the velocity profile is declining in both directions. Dapra et al. [2] discussed perturbation method for the solution of pseudoplastic fluid flow. Hayat et al. [3-4] studied heat transfer effect for a UCM fluid for

different geometrical configurations. Khan et al. [5] discussed Williamson fluid flow behaviour over a stretching sheet. Krishnamurthya et al. [6] proposed the influence of chemical reaction and radiation on MHD Williamson fluid flow over an extending surface. Lyubimov and Perminov et. al. [7] the consequences of gravitational force on a thin layer of a Williamson fluid on an inclined surface were discussed. The numerical solution of the MHD stagnation point flow of Williamson fluid across a stretching cylinder was investigated by Malik et al. [8]. Malik et al. [9] studied homogeneous-heterogeneous interactions in the Williamson fluid model across a stretching cylinder. Monica et al. [12] proposed stagnation point-flow of a Williamson fluid flow over a nonlinearly enlarging sheet. The stagnation point flow for the starching cylinder instance was analyzed by Merkin et al. [11]. Williamson fluid flow via a stretching cylinder and heat transfer along with thermal conductivity and heat generation/absorption have been explored by Malik et al. [10]. Nadeem et al. [13] discussed Williamson fluid flow in two dimensions across a stretched sheet. Nadeem et al. [14] examined the flow of Williamson fluid past a moving surface.

The investigation of temperature stratification as well as heat transfer properties of fluids flowing across a cylindrical surface has received much interest because of its wide range of applications. Some of most important and practical examples associated to applications include manufacture of sheeting material, the thinning of copper wires, and thermal energy storage systems akin to solar ponds etc. Olkha et al. [15-17] investigated non-Newtonian slip flow with heat transfer characteristics due to permeable surface in the presence of magnetic field. Rehman et al. [18] examined heat generation/absorption impact in a dual layered mixed convection flow of Eyring-Powell fluid across an inclined stretched cylinder. Sia et al. [21] explored the numerical analysis of boundary layer flow including heat transfer effects on a stretched porous cylinder. Salahuddin et al. [19] explored the joint impact of thermal conductivity and MHD Williamson fluid flow along a stretching cylinder by utilizing a Keller box method. Sulochana et al. [22] explored influence of heat transfer on dusty nanofluid over a stretched cylinder. They described their outcomes in terms of temperature with extra injection and suction parameters, magnetic field homogeneity, and unique Nano particle shapes. Sattar et al. [20] proposed the behaviour of hybrid nano-liquid flow under the impacts of magnetic field through a porous circular cylinder.

As per the reviewed literature, no research has been done on Williamson fluid flow in a porous medium across a stretching cylindrical surface. Hence, we have given numerical analysis using the R-K 4th order technique in conjunction with the shooting method to address the characteristics of non-Newtonian Williamson fluid flow across a cylindrical surface. The apprehensions of pictorial and tabular notations are used to emphasise the effect of important emerging parameters on both velocity and temperature profiles. The numerical values of the skin friction coefficient and the local Nusselt number are also tabulated.

2. Mathematical formulation

We consider the steady, axisymmetric, incompressible and two-dimensional boundary layer flow of Williamson fluid over a stretching cylinder as shown in Fig.1. The flow is

induced by linear stretching of the surface. The fluid motion is in an axial direction whereas radial direction is perpendicular to it. The continuity, momentum and temperature equations for Williamson fluid model under the usual assumptions associated with the boundary layer flow are (Malik et al. [12])

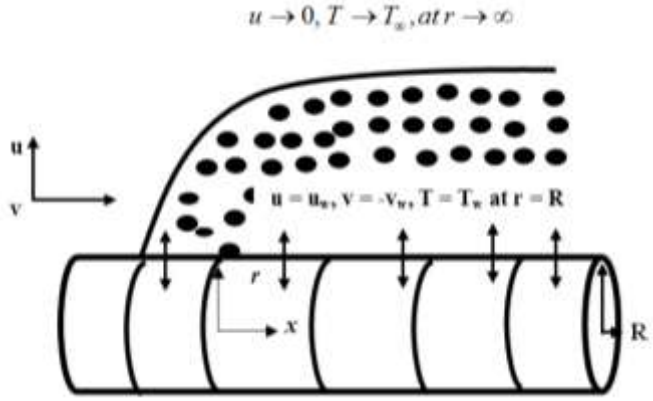

Figure 1. Physical model

$$\frac{\partial(\mathrm{r}\,u)}{\partial x}+\frac{\partial(rv)}{\partial r}=0 \tag{1}$$

$$u\frac{\partial u}{\partial x}+v\frac{\partial u}{\partial r}=\nu\left(\frac{1}{r}\frac{\partial u}{\partial r}+\frac{\partial^2 u}{\partial r^2}\right)+\nu\left(\frac{\Gamma}{\sqrt{2}r}\left(\frac{\partial u}{\partial r}\right)^2+\sqrt{2}\Gamma\frac{\partial u}{\partial r}\frac{\partial^2 u}{\partial r^2}\right)-\frac{\nu}{K_p}u \tag{2}$$

$$u\frac{\partial T}{\partial x}+v\frac{\partial T}{\partial r}=\frac{1}{r}\frac{\partial}{\partial r}(\alpha\,\mathrm{r}\frac{\partial T}{\partial r})+\frac{Q}{\rho C_p}(\mathrm{T}-T_\infty) \tag{3}$$

Here, the velocity components along the flow direction and normal direction are u(r, x) and v(r, x) respectively and $,\nu,\ C_p$, Γ , R are fluid density, kinematic viscosity and specific heat at content pressure, positive time constant and radius of cylinder respectively. T is fluid temperature and T_∞ is ambient fluid temperature.

boundary conditions are follows as

$$\begin{cases} u(\mathrm{x},\mathrm{r})=U=\dfrac{u_0 x}{l}+b_0\nu\dfrac{\partial u}{\partial r}, \\ v(\mathrm{x},\mathrm{r})=-v_w, & at\, r=R \\ T=T_w \end{cases} \tag{4}$$

$$\{u\to 0, T\to T_\infty, \qquad at\, r\to\infty$$

Where $l, T_w, T_\infty,\ v_w, u_0$ are the characteristic length, temperature of surface, the extreme temperature, Suction/injection and reference velocity respectively

Solution:

Proposed association for u, v is represented as

$$\begin{cases} u = \dfrac{1}{r}\dfrac{\partial \psi}{\partial r}, \qquad v = -\dfrac{1}{r}\dfrac{\partial \psi}{\partial x}, \\ \eta = \dfrac{r^2 - R^2}{2R}\sqrt{\dfrac{U}{\nu x}}, \psi = \sqrt{U\nu x} R f(\eta) \\ \theta(\eta) = \dfrac{T - T_\infty}{T_w - T_\infty}, \alpha = \alpha_\infty\left(1 + \varepsilon\theta\right) \end{cases} \tag{5}$$

Here α_∞ denote thermal conductivity at a large distance away from the cylinder.

Equations (2) and (3) are converted to the following non-dimensional form.

$$2\gamma f'' + \left(1 + 2\eta\gamma\right) f''' + \frac{3}{2}\left(1 + 2\eta\gamma\right)^{\frac{1}{2}} \gamma\eta f''^2 + We\left(1 + 2\eta\gamma\right)^{\frac{3}{2}} f'' f''' + f'' f - f'^2 - K_p f' = 0 \tag{6}$$

$$\theta''\left(1 + 2\eta\gamma\right)\left(1 + \varepsilon\theta\right) + \theta'\left(2\gamma + \Pr f + 2\varepsilon\gamma\theta\right) + \theta'^2 \varepsilon\left(1 + 2\eta\gamma\right) + \Pr Q^*\theta = 0 \tag{7}$$

Conditions of Boundary equations (5) reduces as:

$$\begin{cases} f'(0) = 1 + d_1 f''(0) \\ f(0) = S, \\ \theta(0) = 1 \end{cases} \tag{8}$$

$$\left\{ f(\infty) \to 0, \theta(\infty) \to 0, \right.$$

Here $\gamma = \dfrac{1}{R}\sqrt{\dfrac{x\nu}{U}}$: Curvature parameter, $We = \Gamma\sqrt{\dfrac{2U^3}{\nu x}}$: Weissenberg number, $Q^* = \dfrac{Qx}{\rho U C_p}$: Heat generation/absorption parameter, $\Pr = \dfrac{\nu}{\alpha_\infty}$: Prandtl number. ε :

Thermal Conductivity, S; Suction/Injection parameter, $Kp = \frac{\upsilon l}{k_p U_0}$; permeability parameter, d_1; Velocity slip parameter.

The skin friction coefficient is defined as

$$C_f = \frac{\tau_w}{\frac{1}{2}\rho U_w^2}, \tag{9}$$

In the preceding expression τ_w expressed shear stress at the cylinder surface. Shear stress for Williamson fluid is described as

$$\tau_w = \mu\left[\frac{\partial u}{\partial r} + \frac{\Gamma}{\sqrt{2}}\left(\frac{\partial u}{\partial r}\right)^2\right]_{r=R} \tag{10}$$

After putting the *Eq*. (10) in *Eq*. (9) we get following expression

$$C_f \,\mathrm{Re}_x^{\frac{1}{2}} = f''(0) + \frac{We}{2} f''(0)^2 \tag{11}$$

Now the local Nusselt number is defined as

$$Nu_x = \frac{-xq_w}{(T_w - T_\infty)} \text{ where } q_w = -\alpha_\infty \left(\frac{\partial T}{\partial y}\right)\Big|_{r=R}$$

$$Nu_x \,\mathrm{Re}_x^{\frac{-1}{2}} = -\theta'(0), \tag{12}$$

where $\mathrm{Re} = \frac{xu_w}{\upsilon}$: local Reynolds number.

3. Result Discussion

Equations (6-7) subject to boundary condition (8) have been solved numerically by utilizing a MATLAB tool with Runge-Kutta based shooting technique for the distinct value of arising parameters. Computations have been done and the impact of parameters on velocity, temperature, profiles are inspected with the assistance of graphical data. For the verification of current findings with certain activities already completed, a comparative study is carried out. Compared with those of Nadeem et al. [2] Malik et al.

[19] and Observations made depicts that the computed outcomes exhibit outstanding and influential study.

Figures (2-3) represent the prominences of curvature parameter γ on $f(\eta)$ and $\theta(\eta)$ profiles. By improving the γ parameter, $f(\eta)$ and $\theta(\eta)$ profile is increased. So, as we increase the curvature parameter γ , the heat transmission rate speeds up. As a result, as the curvature parameter γ is increased, the $\theta(\eta)$ profile increases. Figure (4) represent the prominences of ε on $\theta(\eta)$ profiles. As increase the ε parameter, $\theta(\eta)$ profile increase.

Figures (5-7) represent the prominences of Weissenberg number We on $f(\eta)$ and $\theta(\eta)$ profiles. By improving the We parameter, $f(\eta)$ profile is increased whereas $\theta(\eta)$ profile gets diminished. Figure (7) represent the prominences of Prandtl number Pr on $\theta(\eta)$ profiles. As increase the Pr parameter, $\theta(\eta)$ profile get cuts down. Lower Pr fluids will have higher thermal conductivity (and thicker thermal boundary layer structures) so that heat can spread from the sheet faster than higher Pr fluids (thinner boundary layers). Prandtl number can be used in conducting flows to increase the cooling rate.

Figure (8) represent the prominences of heat source/sink parameter Q^* on $\theta(\eta)$ profiles. By improving the Q^* parameter, $\theta(\eta)$ profile is increased. Since exothermic reactions and heat release occurred throughout these processes, causing the system's heat to rise and the thermal boundary layer to rise. Figures (9-10) demonstrate the prominences of porous medium parameter Kp on $f(\eta)$ and $\theta(\eta)$ profiles. By improving the Kp parameter, $f(\eta)$ are reduced while that of $\theta(\eta)$ profile is increased.

Figures (7.11-7.12) shows the prominences of velocity slip parameter δ_1 on $f(\eta)$ and $\theta(\eta)$ profiles. By improving the δ_1 parameter, $f(\eta)$ profile gets diminishes whereas the rise is observed in $\theta(\eta)$ profiles This is because of the fact that when the slip parameter increases, slip velocity increase, and consequently, the pulling of the stretching wall can only be partly conveyed to the fluid.

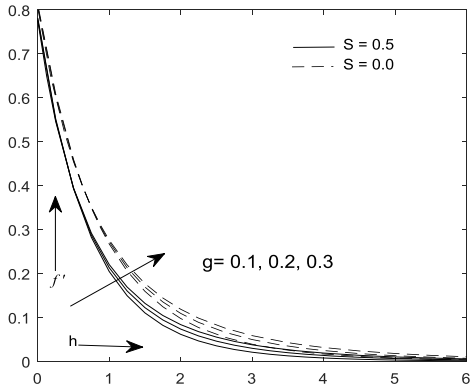

Fig2. Velocity effect for alteration in γ

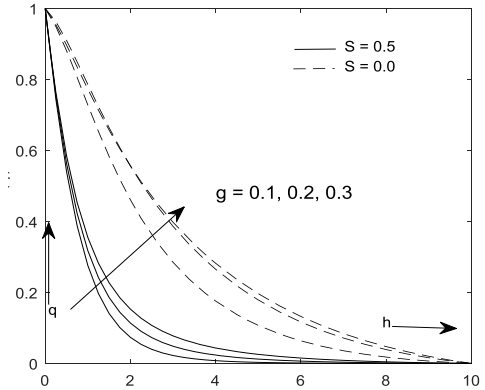

Fig3. Temperature effect for alteration in γ

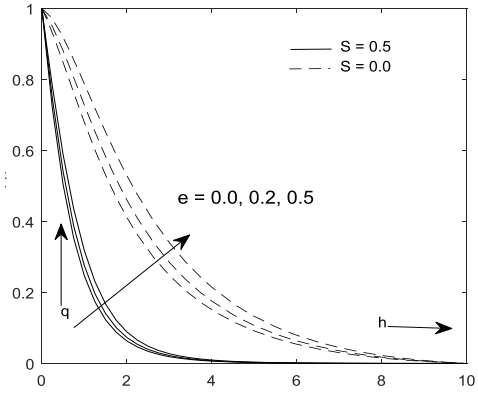

Fig4. Temperature effect for alteration in ε

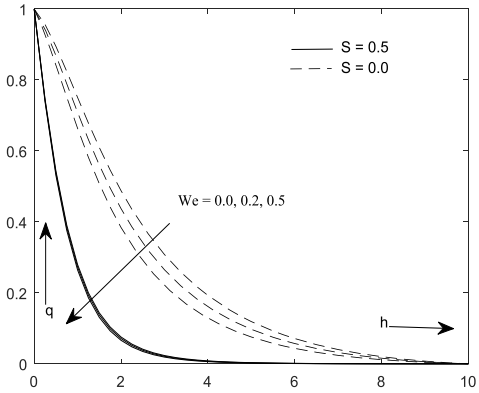

Fig5.Temperature effect for alteration in We

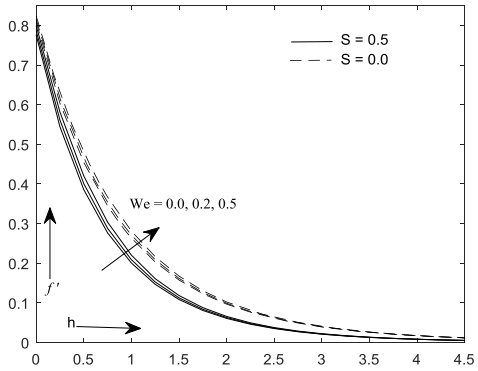

Fig6. Velocity effect for alteration in We

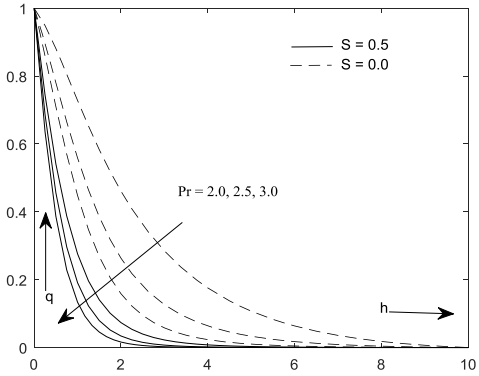

Fig7. Temperature effect for alteration in Pr

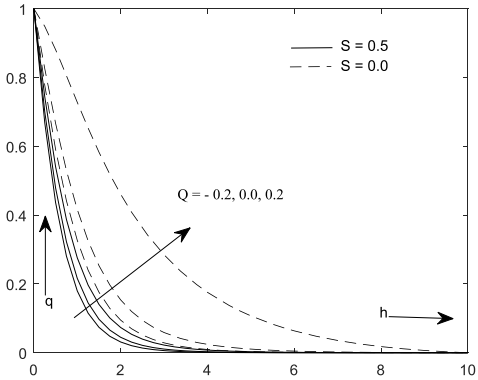

Fig8. Temperature effect for alteration in Q

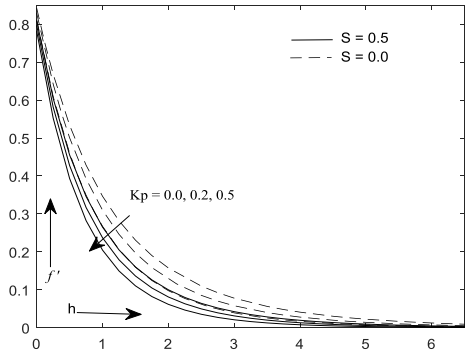

Fig9. Velocity effect for alteration in Kp

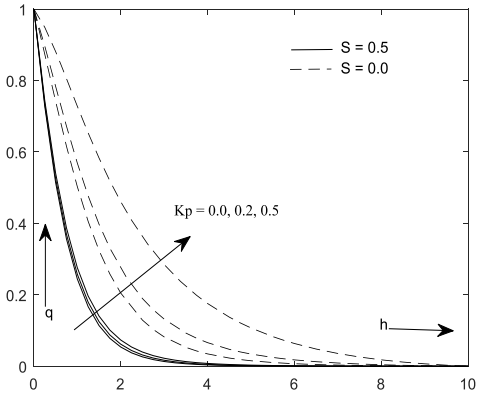

Fig10. Temperature effect for alteration in Kp

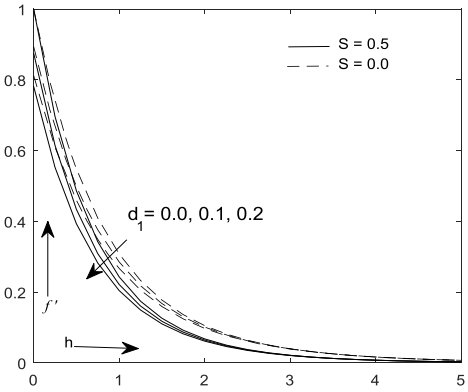

Fig11. Velocity effect for alteration in δ_1

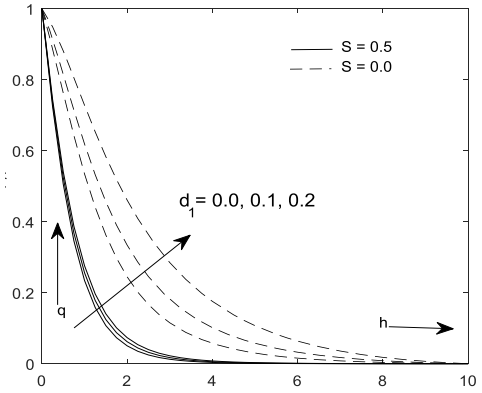

Fig12. Temperature effect for alteration in δ_1

Table -1

Variation of skin friction coefficient C_f , local Nusselt number Nu_x for different value of various parameter with suction.

r	We	ε	Pr	Q	Kp	d_1		$-C_f \, \mathrm{Re}_x^{\frac{1}{2}}$	$Nu \, \mathrm{Re}_x^{\frac{-1}{2}}$
0.1								1.031776359	1.110641725
0.2								1.046109885	1.088095762
0.3								1.060074441	1.067188788
	0.0							1.121754622	1.101049421
	0.2							0.951753398	1.119324813
	0.5							0.751836652	1.141434818
		0.0						1.031776361	1.280750172
		0.2						1.031776359	1.110641725
		0.5						1.031781730	0.916026506
			2.0					1.031776359	1.110641725

			2.5					1.031776361	1.405406208
			3.0					1.031776291	1.685412266
				-0.2				1.031776361	1.534604651
				0.0				1.031776361	1.350480976
				0.2				1.031776359	1.110641725
					0.0			0.908504734	1.192675867
					0.5			0.962788144	1.157342242
					1.0			1.031776359	1.110641725
						0.0		1.342626416	1.191931364
						0.1		1.166323971	1.150201671
						0.2		1.031776359	1.110641725

Table -2

Variation of skin friction coefficient C_f , local Nusselt number Nu_x for different value of various parameter without suction.

r	We	ε	Pr	Q	Kp	d_1		$-C_f \operatorname{Re}_x^{\frac{1}{2}}$	$Nu \operatorname{Re}_x^{\frac{-1}{2}}$
0.1								0.895539821	0.154827308
0.2								0.914116785	0.100068921
0.3								0.931849795	0.140381980
	0.0							0.959005068	0.123994086
	0.2							0.837410493	0.181451693
	0.5							0.686423522	0.244109709
		0.0						0.895541776	0.241524207
		0.2						0.895539821	0.154827308
		0.5						0.895540801	0.059036061
			2.0					0.895539821	0.154827308
			2.5					0.895541595	0.364968580
			3.0					0.895542217	0.511888465
				-0.2				0.895539642	0.943281463
				0.0				0.895539600	0.704849091
				0.2				0.895539821	0.154827308
					0.0			0.757417599	0.472364872
					0.5			0.818204437	0.375824058
					1.0			0.895539821	0.154827308
						0.0		1.141295973	0.405838487
						0.1		1.002543949	0.296506280
						0.2		0.895539821	0.154827308

Table-3 Comparison of skin friction coefficient for different values of We with previous results

We	Nadeem et al.13	Malik et al.9	Present results
0.0	1	1.005	1.00754
0.1	0.976558	0.965285	-
0.2	0.939817	0.927877	0.927675
0.3	0.88272	0.887909	-
0.5	-	-	0.867236

4. Conclusion

In the present analysis, a numerical investigation of flow of Williamson fluid over a stretching cylinder with thermal conductivity and heat generation/absorption is addressed. The influence of numerous quantities on velocity and temperature profile is elaborated graphically in the light of physical interest.

- $f(\eta)$ profile is increasing function of Weissenberg number $\boldsymbol{We}$ and curvature parameter γ .
- $\theta(\eta)$ profile gets diminishes for improving the value of $\boldsymbol{We}$ and **Pr**.
- $\theta(\eta)$ profile enhances for improving the values of thermal conductivity $\boldsymbol{\varepsilon}$ parameter.
- $f(\eta)$ profile gets diminishes with the increasing of slip parameter $\boldsymbol{\delta_1}$ whereas rises the $\theta(\eta)$ profie.

Acknowledgements: The authors are thankful to the Referee for valuable comments and suggestions.

References

[1] Bilal S, Rehman K.U., Malik M.Y., Hussain A, Khan M. (2017). Effects of temperature dependent conductivity and absorptive/generative heat transfer on MHD three-dimensional flow of Williamson fluid due to bidirectional non-linear stretching surface. Results Phys; 7:204-12.

[2] Dapra and Scarpi, G. (2007). Perturbation solution for pulsatile flow of a non-Newtonian Williamson fluid in a rock fracture. Int. J Rock Mech. Min Sci., 44: 271-278.

[3] Hayat, T. Mustafa, M. Shehzad, S. A. and Obaidat, S. (2012), Melting heat transfer in the stagnation-point flow of an upper convected Maxwell (UCM) fluid past a stretching sheet". Int. J. Numer. Meth. Fluids 68, 233-243.

[4] Hayat, T. Iqbal, Z. Mustafa, M. and Alsaedi, A. (2012). Momentum and heat transfer of an upper-convected Maxwell fluid over a moving surface with convective boundary conditions, Nucl. Eng. Des. 252, 242-247.

[5] Khan, M. S. Rahman, M. M. Arifuzzaman, S. M. Biswas, P. and Karim, I. (2017). Williamson fluid flow behaviour of MHD convective radiative cattaneo–

christov heat flux type over a linearly stretched-surface with heat generation and thermal-diffusion," *Frontiers in Heat and Mass Transfer*, 9, 15.

[6] Krishnamurthya, M.R., Prasannakumara, B.C., Gireesha, B.J. Reddy, R.S. (2016). Effect of chemical reaction on MHD boundary layer flow and melting heat transfer of Williamson Nano fluid in porous medium. Engineering Science and Technology, an Int J 19:53-612.

[7] Lyubimov, D.V. and Perminov, A.V. (2002). Motion of a thin oblique layer of a pseudoplastic fluid, Journal of Engineering Physics and Thermophysics 4, 920-924.

[8] Malik, M.Y. and Salahuddin, T. (2015). Numerical solution of MHD stagnation point flow of Williamson fluid model over a stretching cylinder, International Journal of Nonlinear Sciences and Numerical Simulation 16, 161-164.

[9] Malik, M.Y., Salahuddin, T. Arif Hussain, Bilal, S. and Awais, M. (2015). Homogeneous-heterogeneous reactions in Williamsonfluid model over a stretching cylinder by using Keller box method, AIP Advances **5**, 107227.

[10] Monica, M., Sucharitha, J. Kumar, C.K. (2016). Stagnation Point Flow of a Williamson Fluid over a Nonlinearly Stretching Sheet with Thermal Radiation. American Chemical Science Journal 13(4): 1-8, Article no. ACSJ.25144. ISSN: 2249-0205.

[11] Merkin, J.; Najib, N.; Bachok, N.; Ishak, A.; Pop, I. (2017). Stagnation-point flow and heattransfer over an exponentially stretching/shrinking cylinder. *J TAIWAN INST CHEM E 74*, 65-72.

[12] Malik, M. Y., Bibi, M. Farzana Khan, and Salahuddin, T. (2016). Numerical solution of Williamson fluid flow past a stretching cylinder and heat transfer with variable thermal conductivity and heat generation/absorption. AIP Advances 6, 035101; https://doi.org/10.1063/1.4943398.

[13] Nadeem, S. Hussain, S. T. and Lee, C. (2013). Flow of a Williamson fluid over a stretching sheet, *Brazilian Journal of Chemical Engineering*, 30 (3), 619-625.

[14] Nadeem, S. and Hussain, S.T. (2016). Analysis of MHD Williamson nano fluid flow over a heated surface. Journal of Applied Fluid Mechanics, 9 (2):729-739.

[15] Olkha, A. and Dadheech, A. (2021). Unsteady magnetohydrodynamic slip flow of Powell-Eyring fluid with microorganisms over an inclined permeable stretching sheet, J. Nanofluid, Vol. 10, No. 1, pp. 128-145.

[16] Olkha, A. and Dadheech, A., Parmar, A. (2021). Inclined MHD and radiative Maxwell slip flow and heat transfer due to permeable melting surface with a non-linear heat source", Int. J. App. Comput. Math., Vol. 7, No. 89.

[17] Olkha, A. and Dadheech, A. Parmar, A. (2021). MHD slip flow for Casson nanofluid over a radially surface with zero mass flux at the surface, non-linear radiation and temperature jump", IIETA, Vol. 65, No. 1, pp. 129-142, (2021).

[18] Rehman KU, Malik MY, Salahuddin T, Naseer M. (2016). Dual stratified mixed convection flow of Eyring-Powell fluid over an inclined stretching cylinder with heat generation/absorption effect. AIP Adv; 6(7):075112.

[19] Sia, X., Lia, L., Zhenga, L, Zhangb, X. and Liua, B. (2014). The exterior unsteady viscous flow and heat transfer due to a porousexpanding stretching cylinder, Computers and Fluids **105**, 280-284.

[20] Salahuddin, T. Malik, M.Y. Arif Hussain, Bilal, S. and Awais, M. (2015). "Combined effects of variable thermal conductivity and MHD flow on pseudoplastic fluid over a stretching cylinder by using Keller box method," Natural Sciences **5**, 11-19.

[21] Sulochana, C., Sandeep, N. (2016). Flow and heat transfer behavior of MHD dusty nanofluid past a porous stretching/shrinking cylinder at different temperatures. *J APPL FLUID MECH.*

[22] Sattar Dogonchi, A. Tahar Tayebi, Nader Karimi, Chamkha, Ali J. Hesham Alhumade, (2021). Thermal-natural convection and entropy production behavior of hybrid nanoliquid flow under the effects of magnetic field through a porous wavy cavity embodies three circular cylinders, Journal of the Taiwan Institute of Chemical Engineers, ISSN 1876-1070, https://doi.org/10.1016/j.jtice.2021.04.033.